Computer Modelling of Ventricular Rhythm During Atrial Fibrillation and Ventricular Pacing

J Lian, D Müssig, V Lang

Micro Systems Engineering, Inc., Lake Oswego, USA

Abstract

In this paper, we describe a computer model of the ventricular response to atrial fibrillation (AF) in the presence of ventricular pacing (VP). In this model, the AV junction (AVJ) is treated as a lumped structure with defined electrical properties including refractory period and automaticity. The AVJ is randomly bombarded by AF impulses, and can be invaded by the retrograde activation wave induced by the VP as well. The model further incorporates bi-directional conduction delays in both AVJ and ventricle, and the recovery-dependency of the AVJ properties is also considered.

Simulations show that dependent upon model parameter settings, multi-level AF-VP interactions may occur to generate various ventricular rhythms that are consistent with experimental observations. This model may be used to study the mechanism of AF-VP interaction and to develop VP-based ventricular rate smoothing algorithms for ventricular rhythm control during AF.

1. Introduction

The irregular ventricular response during atrial fibrillation (AF) has been explained in terms of decremental conduction and repetitive concealment of the AF impulses within the atrioventricular (AV) node [1,2]. This concept was challenged by the postulate that the AV node functions as a pacemaker whose rate and rhythm are electrotonically modulated by AF impulses, based on the observation that the short RR intervals during AF could be eliminated by ventricular pacing (VP) at relatively long cycle lengths [3,4]. However, such hypothesis was not supported by the experimental data obtained in a dog model, where it was demonstrated the VP cycle length resulting in >95% of ventricular captures during AF was linearly related to the shortest spontaneous RR interval during AF [5]. An alternative hypothesis was the electrotonic modulation of AV node propagation by concealed AF impulses being responsible for the irregular RR intervals during AF [6]. Although the simplified computer models could simulate several features of the ventricular responses during AF, the prediction of inverse relation between the atrial and ventricular rates made from this hypothesis is not compatible with the clinical findings [7]. Moreover, the theoretical RR interval histogram predicted by concealed conduction AF model could not account for many experimental histograms [8].

Another quantitative model for the ventricular response during AF was developed by Cohen et al. [8]. In this model, random AF impulses continuously bombard the AV junction (AVJ), which is treated as a lumped structure with defined electrical properties including refractory period and automaticity. It was demonstrated that this model could adequately account for all the principal statistical properties of the RR intervals during AF [8]. However, several important physiological properties of the heart were not considered in this model, including the conduction delays within AVJ and ventricle, and the recovery-dependency of the AVJ properties. Furthermore, this model did not consider the effects of VP, thus making it difficult to investigate the interaction between AF and VP.

In this study, we describe an enhancement of Cohen's model, by incorporating VP and realistic electrical properties of the heart. We demonstrate through simulations that various experimentally observed patterns of ventricular rhythm during AF and VP may result from multi-level AF-VP interactions.

2. Methods

2.1. Model components

Figure 1 illustrates the schematic drawing of the present computer model, which consists 4 inter-connected components: AF generator, AVJ, ventricle, and electrode.

The AF generator simulates the turbulent electrical activity in the atrium, generating a series of AF impulses bombarding the AVJ. The arrival of the AF impulses is mathematically characterized as a Poisson process with a mean arrival rate λ [8]. Any retrograde penetration of the atrium by an activation wave escaping the AVJ after a retrograde AV delay (see below) collides with an incoming AF impulse, causing the AF generator resets its timing cycle.

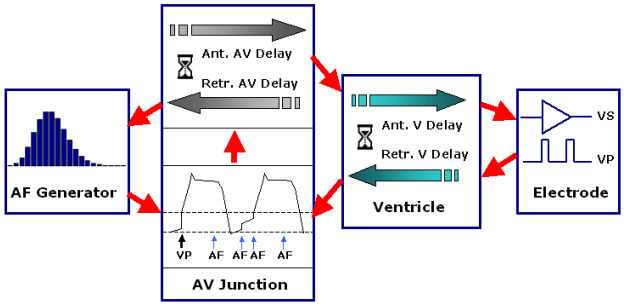

Figure 1. Schematic drawing of the computer model.

As in [8], the AVJ is modeled as a lumped structure characterized by a transmembrane potential V_m, a resting potential V_R, a depolarization threshold V_T, a refractory period τ, and a spontaneous rate V_4 of phase-IV depolarization. Each time when an AF impulse hits the AVJ during phase-IV, V_m increases by a discrete amount ΔV, whereas the retrograde penetration of the AVJ by a VP-induced retrograde wave (see below) during phase-IV brings V_m to V_T immediately. The AVJ fires when V_m reaches V_T as a result of anterograde activation (combined effect of AF bombardment and spontaneous phase-IV depolarization) or retrograde activation. The firing of AVJ generates an activation wave, which starts an anterograde or retrograde AV delay depending upon the direction of activation. Collision within AVJ occurs if AVJ is retrograde activated while an anterograde wave has not finished its AV delay or vice versa. The firing of AVJ also starts a refractory period, during which time the AVJ is refractory to stimulation by both AF impulses and retrograde waves. The V_m returns to V_R and the AVJ restarts phase-IV when refractory period expires.

If an anterograde AV delay expires, an activation wave is generated in the ventricle and starts an anterograde conduction delay (VD_{ant}). The VP also generates an activation wave in the ventricle with a retrograde conduction delay (VD_{ret}), after which period the retrograde wave hits the AVJ. When both anterograde and retrograde ventricle waves are detected, the ventricle fusion beat is predicted, causing extinction of both waves.

The electrode is connected to a pacing device operating in demand mode such as VVI. If an activation wave propagates to the electrode after an anterograde conduction delay, a ventricular sense (VS) occurs that inhibits the scheduled VP, whereas the time out of the ventricular pacing interval (*VPI*) initiates the VP.

2.2. AVJ properties

Besides properties described above, such as spontaneous phase-IV depolarisation and stepwise depolarisation by AF impulses, several other properties of the AVJ are also incorporated in the present model.

First, the refractory period (τ) of the AVJ has been recognized as rate-dependent, such that the slower the heart rate, the longer the τ [8]. We further extend this model by assuming τ depends on the recovery time (T_R) of the AVJ, with their relationship given by:

$$\tau = \tau_{min} + \tau_{ext}(1 - \exp(-T_R / \tau_{ext})) \quad (1)$$

where τ_{min} is the shortest AVJ refractory period corresponding to T_R = 0, and τ_{ext} is the maximum extension of the refractory period when $T_R \to \infty$.

In this model, the recovery time of the AVJ is set to 0 if there is an anterograde or retrograde wave in the AVJ (i.e., AV delay has not expired). Otherwise, it is defined as the interval between the end of the last AVJ refractory period and the current AVJ activation time.

Second, the AV delay (*AVD*) is also known to be dependent on the AVJ recovery time [6,9], and their relationship is modelled by the following equation:

$$AVD = AVD_{min} + \alpha \exp(-T_R / \beta) \quad (2)$$

where AVD_{min} is the minimum AV delay when $T_R \to \infty$, α is the maximum extension of AV delay when T_R = 0, and β is the time constant [9]. The anterograde and retrograde AV delays may share the same set of parameters (as in present simulation study), or these parameters may be independently adjusted for bi-directional AV delays.

Third, the electrotonic modulation of the AVJ refractory period by blocked impulses is also incorporated in our model [6,9]. We denote *tm* the refractory timer starting from the onset of AVJ activation. During AVJ refractory period ($tm < \tau$), any retrograde invasion of the AVJ by VP-induced retrograde wave resets tm = 0. On the other hand, any concealed AF impulse resets *tm* to max(0, tm-δ), where δ is a positive constant. This is equivalent to prolong the AVJ refractory period by up to time interval δ.

2.3. Model parameters

Table 1. Programmable computer model parameters.

Symbol	Unit	Brief description
V_R	*mV*	AVJ resting potential
V_T	*mV*	AVJ activation threshold
ΔV	*mV*	V_m increment by an AF impulse
V_4	*mV/s*	AVJ Phase-IV depolarisation rate
λ	*/s*	Arrival rate of AF impulses
τ_{min}	*s*	Minimum AVJ refractory period
τ_{ext}	*s*	Maximum extension of τ
δ	*s*	Adjustment of τ by concealed AF
AVD_{min}	*s*	Minimum AV delay
α	*s*	Maximum AV delay extension
β	*s*	AV delay extension time constant
VD_{ant}	*s*	Ante. ventricle conduction delay
VD_{ret}	*s*	Retr. ventricle conduction delay
VPI	*s*	Ventricular pacing interval

Table 1 summarizes the basic set of programmable parameters that are included in the present model. As shown in [8], the first 4 parameters actually can be simplified to 2 by considering the relative amplitude of AF impulses and the relative rate of AVJ phase-IV depolarisation. In addition, the present model can be easily extended to consider slight beat-to-beat variations of some parameters (ΔV, τ, etc.), by modelling these parameters with certain statistical distributions.

In the following simulations, the parameters of Table 1 have the following default values unless otherwise specified: V_R=-90mV, V_T=-40mV, ΔV=30mV, V_4=33mV/s, λ=10/s, τ_{min}=0.18s, τ_{ext}=0.1s, δ=0.0s, AVD_{min}=0.07s, α=0.13s, β=0.08s, VD_{ant}=0.05s, VD_{ret}=0.15s, VPI=1.0s.

3. Results

In the absence of VP, the present model is a more general version of Cohen's AF model [8], with additional considerations of the anterograde conduction delays and other AVJ properties (see Section 2.2). Therefore, with proper parameter settings, the present model can account for all the principal statistical properties of the RR interval sequence during AF as shown in [8].

Despite the difference in concept, the present model do provides certain compatibility with the concealed conduction model. The degree of electrotonic modulation of the AVJ refractory period by concealed AF impulses can be adjusted by parameter δ. Using two δ values (0.05s and 0.02s), we investigate the relationship between atrial rate and ventricular rate during AF, by setting AF impulse arrival rate λ to 4, 6, 8, 10, 12, and 14/s, respectively. The mean RR intervals (each averaged over 1000 beats) are plotted against the mean AA intervals in Figure 2.

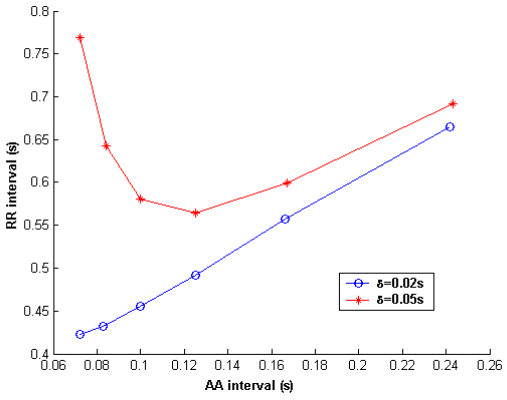

Figure 2. The relationship between atrial and ventricular rates during AF with different degrees of electrotonic modulation by the concealed AF impulses in the AVJ.

Figure 2 shows that in the case of strong electrotonic modulation (δ=0.05s), an inverse relationship between AA intervals and RR intervals is obtained at high AF rate [6,9]. However, in the case of weak electrotonic modulation (δ=0.02s), a positive correlation between atrial rate and ventricular rates is observed [7].

We further investigate the effects of VP on ventricular rhythm during AF. In Figure 3, the *VPI* is respectively set to 0.7, 0.6, 0.5, 0.45, and 0.42s, and 500 RR intervals are plotted for each *VPI* setting. No capture occurs at *VPI*=0.7s, with mean spontaneous RR interval of 0.*417s*. Gradually decreasing *VPI* leads to more paced beats, and the shortest spontaneous RR interval (RR_{min}) being recorded is 0.288s. Note at *VPI*=0.42s, >95% RR intervals are captured by VP, with the difference between *VPI* and RR_{min} greater than 0.13s [3-6].

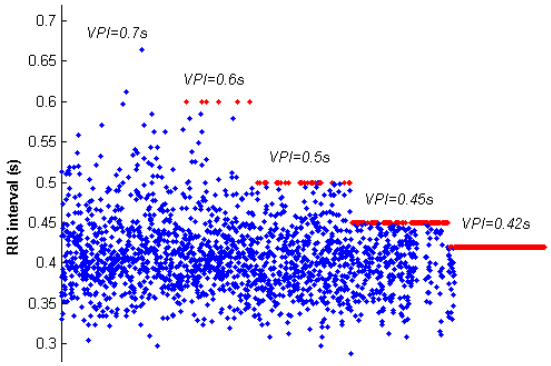

Figure 3. Plot of RR intervals with different *VPI* settings for slow spontaneous ventricular rate (default λ and ΔV).

Figure 4 shows another example, in which case λ=22/s, ΔV =50mV. The mean spontaneous RR interval is 0.224s, and the *VPI* is set to 0.3, 0.28, 0.26, 0.24, and 0.22s, respectively. Note that >95% RR intervals are captured at *VPI*=0.22s, whose difference with RR_{min} (0.181s) is less than 0.04s [5,6].

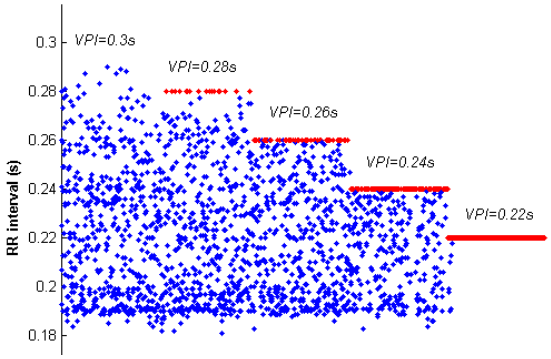

Figure 4. Plot of RR intervals with different *VPI* settings for fast spontaneous ventricular rate (λ=22/s, ΔV=50mV).

To further illustrate the interactions between AF and VP, Figure 5 plots the beat percentage of VP-induced retrograde waves that penetrate and extinct in atrium, ventricle, and AVJ, respectively, with fixed ΔV=40mVand *VPI*=0.4s, while varying AF rate by setting λ to 6, 8, 10, 12, 14 and 16/s, respectively.

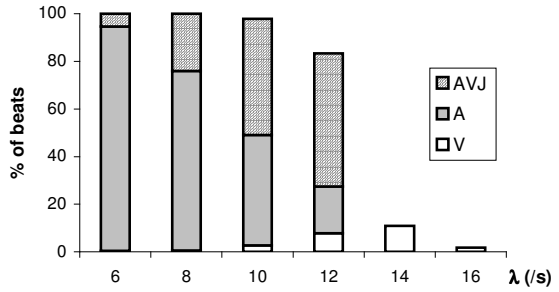

Figure 5. Beat percentage of VP-induced retrograde waves that penetrate and extinct in atrium (A), ventricle (V), and AVJ, respectively, with varying AF rate (λ).

At slow AF rate (λ=6, 8/s), VP captures all beats, and most VP-induced retrograde waves penetrate the atrium and reset the AF generator, while a small portion of retrograde waves collide with AF-induced anterograde waves in the AVJ. As AF rate increases (λ=10, 12/s), most collisions occur in the AVJ while less retrograde waves can penetrate the atrium. Meanwhile, some anterograde waves are able to reach the ventricle and fuse with the VP-induced retrograde waves, or generate sensed beats. Further increasing AF rate (λ=14, 16/s) causes more sensed beats, and all paces lead to fusion beats in the ventricle. Our results further show that increasing AF rate is associated with decreasing AVJ recovery time, with mean T_R (average for AVJ activations in 500 beats) of 0.143, 0.139, 0.131, 0.123, 0.110, and 0.097s, corresponding to the above 6 AF rates, respectively. We also found that at very high pacing rate (for example set VPI=0.2s), all VP-induced retrograde waves are blocked by the refractory AVJ.

4. Discussion

It has been demonstrated that the irregular ventricular rhythm during AF could be stabilized by properly programmed VP [3,4], but the underlying mechanisms remain unclear and controversies exist [1-6].

In this study, the previously developed AF model [8] is enhanced to demonstrate and elucidate the effects of VP on the ventricular rhythm during AF. In this model, the random AF impulses continuously bombard the AVJ, which has a spontaneous rate of phase-IV depolarisation, and can be depolarised by VP-induced retrograde wave as well. Realistic properties of the heart, including bi-directional conduction times in both AVJ and ventricle, are also incorporated in our model. In addition, the dependency of AVJ refractory period and conduction delay on AVJ recovery time is considered. We further provide this model a feature to simulate the electrotonic modulation of the AVJ refractory period by concealed impulses. Therefore, this model represents a unified platform of previous models [1-6,8,9].

Our simulations showed that dependent upon model parameter settings, the VP-induced retrograde wave: (1) may fuse with the anterograde wave at ventricle, (2) may be blocked by the refractory AVJ, (3) may intercept the anterograde wave at AVJ, and (4) may penetrate the atrium and reset the AF generator. Such multi-level AF-VP interactions may generate various RR interval patterns that can account for all previous observations [3-9].

This model may provide insight into the mechanism of AF-VP interaction, and can be used to develop VP-based ventricular rate smoothing algorithms for ventricular rhythm control during AF.

Acknowledgements

The authors wish to thank Dr. S E Greenhut for helpful discussions on the atrial fibrillation computer model.

References

[1] Langendorf R. Concealed AV conduction: the effect of blocked impulses on the formation and conduction of subsequent impulses. Am Heart J 1948; 35:542-52.

[2] Watanabe Y, Watanabe M. Impulse formation and conduction of excitation in the atrioventricular node. J Cardiovasc Electrophysiol 1994; 5:517-31.

[3] Wittkampf FH, de Jongste MJ, Lie HI, Meijler FL. Effect of right ventricular pacing on ventricular rhythm during atrial fibrillation. J Am Coll Cardiol 1988; 11:539-45.

[4] Wittkampf FH, de Jongste MJ, Meijler FL. Atrioventricular nodal response to retrograde atrio-ventricular activation in atrial fibrillation. J Cardiovasc Electrophysiol 1990; 1:437-47.

[5] Vereckei A, Vera Z, Pride HP, Zipes D. Atrioventricular nodal conduction rather than automaticity determines the ventricular rate during atrial fibrillation and atrial flutter. J Cardiovasc Electrophysiol 1992; 3:534-43.

[6] Meijler FL, Jalife J, Beaumont J, Vaidya D. AV nodal function during atrial fibrillation: the role of electrotonic modulation of propagation. J Cardiovasc Electrophysiol 1996; 7:843-61.

[7] Asano Y, Saito J, Yamamoto T, Uchida M, Yamada Y, Matsumoto K, Matsuo H. Electrophysiologic determinants of ventricular rate in human atrial fibrillation. J Cardiovasc Electrophysiol 1995; 6:343-9.

[8] Cohen RJ, Berger RD, Dushane TE. A quantitative model for the ventricular response during atrial fibrillation. IEEE Trans Biomed Eng, 1983; 30: 769-81.

[9] Jorgensen P, Schafer C, Guerra PG, Talajic M, Nattel S, Glass L. A mathematical model of human atrioventricular nodal function incorporating concealed conduction. Bull Math Biol 2002; 64:1083-99.

Address for correspondence.

Jie Lian, Ph.D.
Micro Systems Engineering, Inc.
6024 SW Jean Rd., Lake Oswego, OR 97035
Email: jie.lian@biotronik.com